

## Observation of ordered structures for S/Cu(111) at low temperature and coverage

Erik Wahlström, Inger Ekvall, Håkan Olin, Stig-Åke Lindgren, and Lars Walldén

*Physics and Engineering Physics, Chalmers University of Technology and Göteborg University, SE-412 96 Göteborg, Sweden*

(Received 14 June 1999)

Via scanning tunneling microscopy and low energy electron loss diffraction we observe ordered low-temperature surface structures for S/Cu(111) at low-S coverage and characterize the system also with core level photoemission. The first structure to appear upon S deposition is honeycomblike with a large mesh [ $(\sqrt{43} \times \sqrt{43})R \pm 7.5^\circ$ ], a large nearest S-S distance ( $\sim 4 \text{ \AA}$ ) and low-ordering temperature ( $< 170 \text{ K}$ ). Islands of this structure are observed at low coverage ( $\theta \sim 0.05$ ) and at  $\theta \sim 0.25$  nearly all of the surface area is covered. [S0163-1829(99)07139-8]

Historically the study of S surface structures on Cu(111) has been motivated by the poisoning by S of Cu-based catalysts.<sup>1</sup> For Cu(111) the early low-energy electron diffraction (LEED) observations by Domange and Oudar<sup>2</sup> revealed two different room temperature (RT) structures appearing in succession as the S coverage is increased. These experiments and numerous later ones<sup>1-7</sup> were made with the sample kept at or above RT. At temperatures in this range the S deposition can be made by exposing the sample to H<sub>2</sub>S. The two structures are rather complicated consisting, according to the interpretation of scanning tunneling microscopy (STM) images and x-ray diffraction data, of an uppermost layer of Cu<sub>4</sub>S building blocks and with S atoms also in sites beneath the tetramers.<sup>4,5</sup> Here, we show that, if the sample is cooled after S deposition, the development of ordered structures can be monitored from an earlier stage. STM images show that already at low-S coverages there are islands formed by protrusions organized in a honeycomblike ( $\sqrt{43} \times \sqrt{43})R \pm 7.5^\circ$  structure (here labeled the hc structure) with a disordering temperature of around 150 K. That it is an order-disorder transition, which occurs at this temperature is supported by high resolution S2*p* core level data. When more S is added to the sample prior to cooling, the hc structure remains, although compressed, as a background pattern to new higher protrusions. It is only after these structures have formed that additional deposition gives the two previously studied RT structures. Aside from the observation that the new structures appear via the ordering of a species present also at higher temperature, the existence of additional S/Cu(111) structures at low temperature and coverage is of little significance for understanding the catalytic properties of the system. Instead the structures, particularly the hc structure, are of interest per se. The very long interatomic distances and the open honeycomb arrangement indicates that long as well as short-range forces must be included to explain the hc structure. Structure predictions based on first principles total energy calculations is of strong present interest and the hc structure provides a challenge for these.

We first observed the new structure in STM images, but we have also observed LEED patterns and recorded core-level binding energies for the S/Cu(111) system. Most of the work has been devoted to STM observations of the hc structure. For this we have used a commercial variable temperature STM (Omicron GmbH) with W tips.<sup>8</sup> All tunneling volt-

ages in this paper are given as sample voltages relative to the tip. The core level binding energies were determined via photoemission measurements at BLI311 in the MAX-laboratory (Lund Univ.). The S surface densities,  $\theta$ , given below are in units of the surface density of Cu(111). The values are obtained using as a reference the coverage of  $\theta = 0.35$  for the  $\begin{vmatrix} 4 & 1 \\ -1 & 4 \end{vmatrix}$  structure (hereafter denoted the zig-zag structure).<sup>1,4</sup> In addition to this we have assumed that the sticking coefficient is constant for  $\theta < 0.35$ , so that exposures can be converted into coverage. Support for this is obtained from earlier Auger intensity studies,<sup>1</sup> and from the S 2*p* core-level intensity, which is found to increase linearly with exposure in this range.

In our RT images of the clean Cu(111) crystal the close-packed lattice of the surface is resolved and we also observe Friedel oscillations in the surface-state density near step edges and around defects.<sup>9,10</sup>

Upon H<sub>2</sub>S exposure resulting in a S coverage of  $\theta \sim 0.05$  the images change. The step edges are aligned along the  $\langle 011 \rangle$  directions of the substrate lattice. As can be seen in Fig. 1 lower inset, step edges and dislocations found at the surface are decorated by protrusions separated by 5.1 Å, twice the interatomic distance of the Cu(111) lattice. At some edges the protrusions also form equilateral triangles with an average side length of  $\sim 30 \text{ \AA}$ . The step edges can change position during scanning at RT. The triangles located at the edges may also change in both size and position, especially at low resistance setpoints when such triangles occasionally are created on plateaus by the scanning process. On the terraces the image quality deteriorates after exposure. The Cu(111) lattice could however still be resolved.

If the sample is cooled below 170 K after a dose in the range between one fifth and two thirds of that required to obtain the zig-zag structure ( $\theta \sim 0.07-0.25$ ), the observations are significantly different. Of main interest is that instead of a streaky image of the terraces, these are in part covered by an ordered structure (Fig. 2). The area covered is roughly linear with H<sub>2</sub>S exposure, with almost the whole surface covered at  $\theta \sim 0.25$ . Outside the covered parts the Cu(111) lattice can be resolved, and at low temperatures,  $\sim 50 \text{ K}$ , the image quality is comparable to that of clean Cu(111) images. The pattern is hexagonal with a large,  $(16.7 \pm 0.4) \text{ \AA}$ , lattice parameter (Fig. 3). Analysis of the STM images as well as the LEED patterns, shows that the

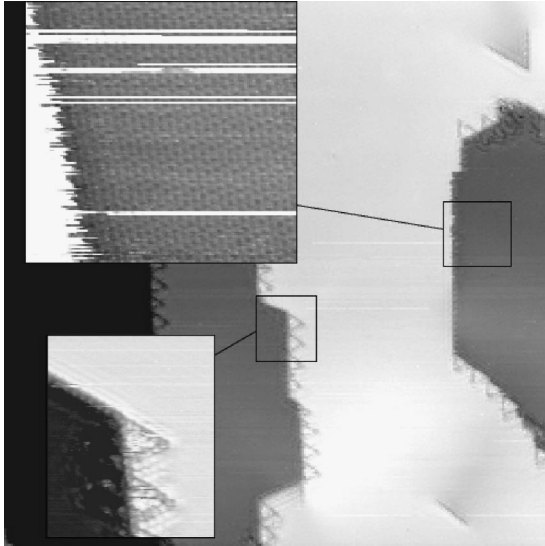


FIG. 1. STM image of S/Cu(111) at  $\theta \sim 0.1$  and RT. The alignment of the step edges along the  $\langle 011 \rangle$  directions can be seen, as well as the decoration of the step edges with protrusions and triangles. The top inset shows a close-up of an edge at low resistance set-point which reveals the characteristic close-packed Cu(111) lattice, while the bottom inset shows the decoration of a step edge.  $I = 0.5$  nA,  $U = -0.946$  V, size  $1000 \times 1000 \text{ \AA}^2$ . Top inset:  $I = 0.197$  nA,  $U = -0.020$  V, size  $80 \times 80 \text{ \AA}^2$ . Bottom inset:  $I = 0.173$  nA,  $U = -0.981$  V, size  $100 \times 130 \text{ \AA}^2$ .

structure is rotated by  $(7.5 \pm 1)^\circ$  with respect to the underlying Cu lattice. The images show hexagonally placed depressions, which are separated by walls with a height of  $(0.7 \pm 0.2) \text{ \AA}$  and an average width of about  $9 \text{ \AA}$  [at bias voltages in the range of  $(0.3-2) \text{ V}$ ]. The bottoms of the

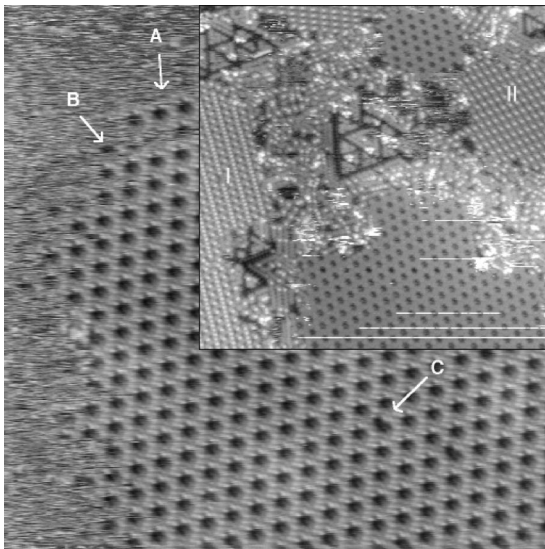


FIG. 2. STM image of S/Cu(111) at  $\theta \sim 0.15$ . The  $(\sqrt{43} \times \sqrt{43})R \pm 7.5^\circ$  can be seen covering parts of a terrace, the arrows mark: A—a wall termination, B—a hole termination, C—a defect in the lattice.  $T = 140$  K,  $I = 0.147$  nA,  $U = -1.00$  V, image size  $400 \times 400 \text{ \AA}^2$ . The inset shows the surface after exposure to further  $\text{H}_2\text{S}$ ,  $\theta \sim 0.3$ , two other patterns (I and II) can be seen together with the  $(\sqrt{43} \times \sqrt{43})R \pm 7.5^\circ$  pattern.  $T = 135$  K,  $I = 0.183$  nA,  $U = -1.178$  V, size  $350 \times 350 \text{ \AA}^2$ .

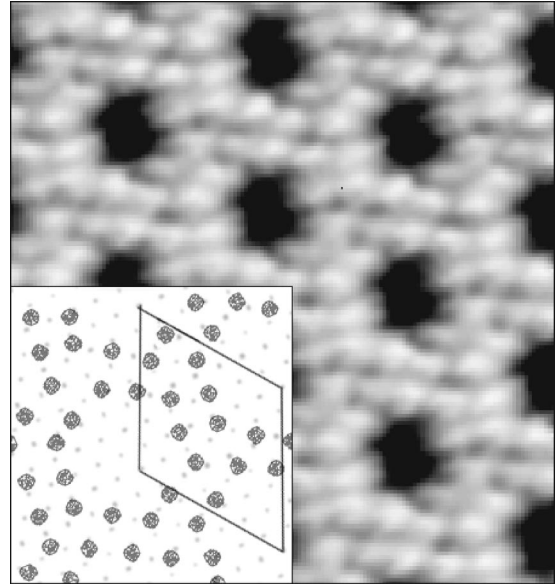


FIG. 3. Close-up of the  $(\sqrt{43} \times \sqrt{43})R \pm 7.5^\circ$ -structure  $T = 135$  K  $I = 0.100$  nA,  $U = -0.700$  V, size  $50 \times 50 \text{ \AA}^2$ . The inset shows the positions of the protrusions (large spots), for comparison drawn together with the Cu(111) lattice (faint spots).

troughs are at about the same height as the substrate. Often a small protrusion (height  $\sim 0.2 \text{ \AA}$ ) can be found in the center of a depression. The areas covered by the ordered structure can be found both next to a step edge or isolated on a plateau. Even with high tunneling resistances (tenths of  $\text{G}\Omega$ ), the boundaries of the structure are not stable during scanning. From one image to the next changes could be seen at length scales from single protrusions to the unit cell length. This effect decreases drastically at lower temperatures. The boundary of the area covered by the ordered structure can be either a wall or a depression (arrows A and B, respectively in Fig. 2). Defects in the structure can also be seen (arrow C in Fig. 2). The wall or part of the wall between two adjacent troughs may be absent and this defect sometimes shifts position from one cell to the next between two images.

A lattice commensurate with the Cu(111) lattice that fits well with the unit cell described above, and with the LEED pattern for coverages below  $\theta \sim 0.25$  can be annotated  $(\sqrt{43} \times \sqrt{43})R \pm 7.5^\circ$ . The apparent height of the protrusions of the wall changed, depending on tip status and bias voltage. In a well-resolved image like Fig. 3, 12 protrusions can be seen forming a hexagon around each depression. It is interesting to note that it is not possible to fit the positions of the protrusions with any single high-coordination sites of the substrate lattice.

To study the influence of temperature on the structure we raised the temperature from 140 to 170 K slowly enough ( $\sim 0.5 \text{ K/min}$ ) to study the dissolution of the hc structure. During this process areas covered by the structure gradually diminish and disappear. The STM images are then similar to those obtained at RT. Upon recoiling, the structure reappears at  $\sim 150$  K, though not always in the same areas as before. Also the LEED pattern shows a reversible transition. The step edges and the triangular defects at the step edges do not change during this temperature cycling, which suggests that no mass transport to or from the step edges is involved

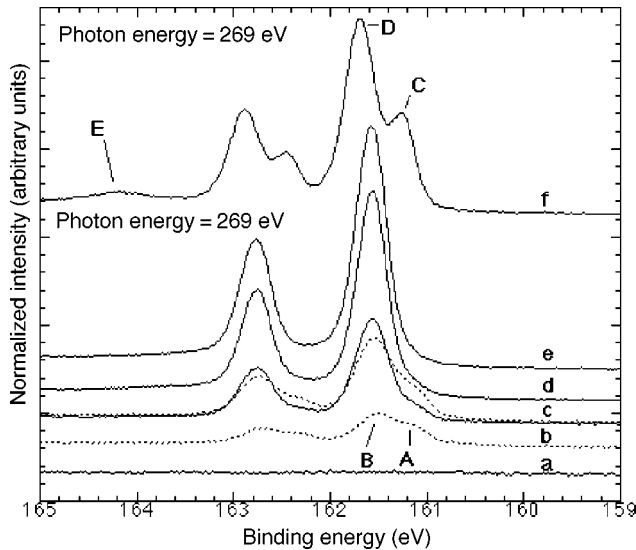


FIG. 4. Photoelectron energy spectra for the S  $2p$  levels at different coverages. The full lines are from cold samples  $\sim 100$  K, while the broken lines are for the RT sample. (a)  $\theta \sim 0$ , (b)  $\theta \sim 0.05$ , (c)  $\theta \sim 0.2[(\sqrt{43} \times \sqrt{43})R \pm 7.5^\circ]$ , (d)  $\theta \sim 0.3$  (just before the zig-zag structure forms), (e)  $\theta \sim 0.35$  (zig-zag structure), (f)  $\theta \sim 0.4[(\sqrt{7} \times \sqrt{7})R \pm 19^\circ]$ . E is the S  $2p_{3/2}$  peak due to  $\text{H}_2\text{S}$  adsorbed on the cold sample.

in the formation of the structure.

For  $\theta > 0.25$  the hc pattern is gradually replaced by new structures (inset Fig. 2), which cover the surface completely at  $\theta \sim 0.3$ . These structures are more compact than the  $(\sqrt{43} \times \sqrt{43})R \pm 7.5^\circ$  pattern. One pattern observed is similar to the hc structure, but has a shorter lattice parameter ( $\sim 11$  Å) and is aligned with the substrate lattice (I in Fig. 2). Two other keep the rotation of the hc structure in one direction but are distorted in other directions (II in Fig. 2). These structures are more resistant to heating, and disappear only above  $\sim 250$  K. For all of these structures a fraction of the protrusions are higher, extending  $(0.5 \pm 0.3)$  Å above those of the hc structure.

For coverages at or above  $\theta \sim 0.35$ , we observe in turn the zig-zag structure and the  $(\sqrt{7} \times \sqrt{7})R \pm 19^\circ$  reconstruction ( $\theta \sim 0.4$ ) studied in earlier work.<sup>1,5</sup> Our RT images of these are quite similar to those reported. Lowering the temperature (125 K) has no marked influence on the images of these.

Via the number of S  $2p$  spin-orbit doublets resolved in photoemission spectra (Fig. 4) three different coverage ranges are identified. At low coverage there are two S  $2p_{3/2}$  levels (A and B in Fig. 4) of which only B remains at intermediate coverage and is replaced by two peaks (C and D) as the S saturation  $[(\sqrt{7} \times \sqrt{7})R \pm 19^\circ]$  structure forms. A and B are separated by  $\sim 0.4$  eV, C and D by 0.44 eV. At the photon energy (269 eV) used to record the spectra in Fig. 4 peak D is twice as intense as peak C. This intensity ratio is also the mean value for the relative intensities measured at six different photon energies between 220 eV and 643 eV. Due to diffraction effects the ratio varies with photon energy<sup>11</sup> around an average value, which should reflect the relative occupancy of the different sites. According to x-ray diffraction results<sup>4</sup> the  $(\sqrt{7} \times \sqrt{7})R \pm 19^\circ$  structure contains two subsurface S atoms for every S surface atom. The present core level data are thus consistent with this provided

the low-binding energy peak is ascribed to the topmost S atoms. Regarding the low-coverage results, we ascribe the shoulder A to sulfur atoms associated with the triangles and decorations of the step edges. Like shoulder A these structures are only observed at low coverages, before the zig-zag structure forms. The observation of only one S  $2p_{3/2}$  peak for the hc structure, is consistent with the STM images where the protrusions appear with similar height and area. For an S coverage between that of the hc pattern and the  $(\sqrt{7} \times \sqrt{7})R \pm 19^\circ$  structure, STM images (like the inset in Fig. 2) and x-ray diffraction data<sup>4</sup> for the zig-zag pattern suggest that there are different sites for the S atoms, but evidently the binding energy difference between these is too small to be resolved. Thus, from the core level data it seems that the zig-zag structure is more related to the hc structure and the intermediate structures than to the  $(\sqrt{7} \times \sqrt{7})R \pm 19^\circ$  structure.

Apart from a thermal broadening (see curve c in Fig. 4) the core-level spectra are not significantly affected by temperature in the probed range. This indicates that formation of the hc and the zig-zag structure involves no major reordering of the S atoms.

In STM images of the structures following the hc lattice there are protrusions with different heights. There are two possible reasons for this, (a) restructuring or (b) local density of state changes at the surface, resulting in different apparent heights for different S atoms. However at this point we do not have enough information to model the atomic structures of the  $(\sqrt{43} \times \sqrt{43})R \pm 7.5^\circ$  structure, and the following structures. We can therefore give no answer to the origin of the higher protrusions in the STM images of higher coverages than  $\theta \sim 0.25$ .

An obvious interpretation of the observations is that the hc structure is built by a species which is present on the terraces also at RT but then in disordered form, and too mobile to be captured in the STM images. The identity of the species can not be determined with certainty. We note, however, that 12 protrusions in the unit cell, gives a surface density of 0.28. This is close to the value of  $\sim 0.25$ , obtained from the  $\text{H}_2\text{S}$  exposures for the S coverage at which nearly the whole surface is covered with the hc structure. There is thus one protrusion for every S atom deposited. The building unit may, therefore, be a S atom, an adsorbed one or one with another entourage of Cu atoms, but it might also be a  $\text{S}_n$  molecule. What makes the latter possibility worthy of consideration is that an open hc structure is unusual for atomic adsorbates, and that the 12 hexagonally arranged protrusions has a likeness to the ring shape of S molecules. Of these  $\text{S}_{12}$ , next to  $\text{S}_8$ , is the most stable one.<sup>12</sup> The molecular bond length is however only half of the  $\sim 4$ -Å distance between the surface protrusions. Furthermore the molecular rings are puckered whereas the STM images indicate that the protrusions are in one plane. A considerable bond length increase and bond strength decrease is expected upon adsorption, as discussed for oxygen molecules interacting with noble and transition metal surfaces.<sup>13</sup> However, since the nearest distance between protrusions in adjacent hexagons is similar to the nearest distance in one hexagon, one would expect the inter- and intra-hexagon bonds to break at approximately the same temperature. We, therefore, believe that the structure is

built from smaller units. Experimentally an indication of this is given by the incomplete hexagons observed at the edges of the hc islands (Fig. 2, arrow B).

The large open areas of the hc structure is interesting since they may be the result of long-ranged substrate mediated interactions. One such example is the interaction mediated by an elastic distortion of the substrate. The interaction energy is estimated to be about 0.1 eV for ordinary interatomic distances and to fall off like  $1/R^3$  (Ref. 14). Recently the formation of S clusters for S/Re(0001) has been attributed to these forces.<sup>15</sup> Another long-ranged interaction of importance is the one mediated by the Cu(111) surface state electrons. This Friedel interaction has been suggested to be important for the positioning of unknown impurities in the surface layer of the Cu(111).<sup>10</sup> The interaction is oscillatory with a period length of half the Fermi wavelength [ $15 \text{ \AA}$  at the Cu(111) surface], which is close the period of the hc structure. At least for a half-filled surface band the density oscillations are expected to give an interaction energy large enough to be of interest for low temperature structures.<sup>16</sup>

Previously for atomic adsorbates it has been possible to account for observed structures by total energy calculations.

We expect this to be rather demanding for the hc structure. The unit cell is large and furthermore the nearest neighbor distance is big enough for long-range interactions to be important. To reproduce the charge density for the Cu(111) substrate by using standard slab calculations the unit cell must contain many planes of Cu atoms. Less demanding, but helpful for understanding the structure and its formation would be to see whether a preferred coordination for single S atoms on Cu(111) can be predicted. From the present data the coordination of the S atoms can not be determined with confidence. That the S  $2p$  binding energy of the hc structure is intermediate between the binding energies of the buried atoms and the surface atoms of the  $(\sqrt{7} \times \sqrt{7})R \pm 19^\circ$  structure suggests that also the coordination is intermediate.

In summary, we have observed for S/Cu(111) a  $(\sqrt{43} \times \sqrt{43})R \pm 7.5^\circ$  structure at low temperature ( $< 170 \text{ K}$ ) and coverage ( $\theta < 0.25$ ). The structure transforms to a disordered phase at  $T = 150 - 170 \text{ K}$ .

We thank Jesper Andersen for helpful advice regarding photoemission measurements. This work has been supported by the Swedish Natural Science Research Council.

<sup>1</sup>C. Campbell and B. Koel, Surf. Sci. **183**, 100 (1987).

<sup>2</sup>J. Domange and J. Oudar, Surf. Sci. **11**, 124 (1968).

<sup>3</sup>N. Prince, D. Seymore, M. Aswin, C. McConville, and D. Woodruff, Surf. Sci. **230**, 13 (1990).

<sup>4</sup>M. Foss, R. Feidenhans'l, M. Nielsen, E. Findeisen, T. Buslaps, R. Johnson, and F. Besenbacher, Surf. Sci. **388**, 5 (1997).

<sup>5</sup>L. Ruan, I. Stensgaard, F. Besenbacher, and E. Laegsgaard, Ultramicroscopy **42-44**, 498 (1992).

<sup>6</sup>K. Motai, T. Hushizume, H. Lu, D. Jeon, and T. Sakurai, Appl. Surf. Sci. **67**, 246 (1993).

<sup>7</sup>S. Rousset, S. Gauthier, O. Siboulet, W. Sacks, M. Belin, and J. Klein, Phys. Rev. Lett. **63**, 1265 (1989).

<sup>8</sup>I. Ekvall, E. Wahlström, D. Claesson, H. Olin, and E. Olsson,

Meas. Sci. Technol. **10**, 11 (1999).

<sup>9</sup>M. Crommie, C. Lutz, and D. Eigler, Nature **363**, 524 (1993).

<sup>10</sup>E. Wahlström, I. Ekvall, H. Olin, and L. Walldén, Appl. Phys. A: Mater. Sci. Process. **66**, S1107 (1998).

<sup>11</sup>F. Strisland, A. Beutler, A. Jaworowski, R. Nyholm, B. Setlik, D. Heskett, and J. Andersen, Surf. Sci. **410**, 330 (1998).

<sup>12</sup>B. Meyer, Chem. Rev. **76**, 367 (1976).

<sup>13</sup>L. Lou, P. Nordlander, and B. Hellsing, Surf. Sci. **320**, 320 (1994).

<sup>14</sup>K. Lau and W. Kohn, Surf. Sci. **65**, 607 (1977).

<sup>15</sup>R. Hwang, D. Zelingski, A. V. de Parga, D. Ogletree, G. Somorjai, and M. Salmeron, Phys. Rev. B **44**, 1914 (1991).

<sup>16</sup>K. Lau and W. Kohn, Surf. Sci. **75**, 69 (1978).